# Dissolved Organic Matter and Associated Trace Metal Dynamics from River to Lake, Under Ice-Covered and Ice-Free Conditions

Worms, Isabelle; Chmiel, Hannah E.; Traber, Jacqueline; Tofield-Pasche, Natacha; Slaveykova, Vera

**Supporting Information**

# Dissolved Organic Matter and Associated Trace Metal Dynamics from River to Lake, Under Ice-covered and Ice-free Conditions

*Isabelle A. M. Worms[1*], Hannah E. Chmiel[2], Jacqueline Traber[3], Natacha Tofield-Pasche[2] and Vera I. Slaveykova[1*]*

[1]Environmental Biogeochemistry and Ecotoxicology, Department F.-A. Forel for environmental and aquatic sciences, Earth and Environmental Sciences, Faculty of Sciences, University of Geneva, 66, boulevard Carl-Vogt, CH-1211 Geneva, Switzerland

[2] Limnological Center, Ecole Polytechnique Fédérale de Lausanne (EPFL), Station 2, 1015 Lausanne, Switzerland

[3] Process Engineering, Eawag, Überlandstrasse 133, 8600 Dübendorf, Switzerland

*corresponding authors

tel: + 41 22 379 05 90; +41 22 379 03 35

e-mail: isabelle.worms@unige.ch; vera.slaveykova@unige.ch

**Number of Pages: 21**
**1 Supplementary Material, 3 Sections, 6 Figures, 4 Tables**

## Table of contents



## List of Figures



## List of Tables

## Section 1: Lake Onega, sampling sites and main characteristics of the Bay hydrochemistry under ice-covered and ice-free conditions

**Table S1.** Abbreviation list of the sampling sites, location according to Figure S1, coordinates and sampling depths for March and June 2017 campaigns.

| Station | Name and Location | Coordinates | Sampling depth (m) |
|---|---|---|---|
| **March 2017** | | | |
| SR | Shuya River | N61 50.830 E34 21.454 | 0.5 |
| S2 | Site 2 Petrozavodsk Bay | N61 49.613 E34 22.195 | 0.5, 15.5, 21 |
| S3 | Site 3 Petrozavodsk Bay | N61 48.826 E34 25.600 | 0.5, 18.5, 27.5 |
| S4 | Site 4 Petrozavodsk Bay | N61 46.707 E34 31.797 | 1, 18.5, 30 |
| **June 2017** | | | |
| SR | Shuya River | N61 50.830 E34 21.454 | 1 |
| S2 | Site 2 Petrozavodsk Bay | N61 49.600 E34 22.258 | 1, 10, 21 |
| S3 | Site 3 Petrozavodsk Bay | N61 48.447 E34 26.018 | 1, 19, 25 |
| S4 | Site 4 Petrozavodsk Bay | N61 46.707 E34 31.797 | 1, 10, 30 |
| S5 | Site 5 Lake Onega | N61 41.937 E34 58.995 | 1, 20, 40 |

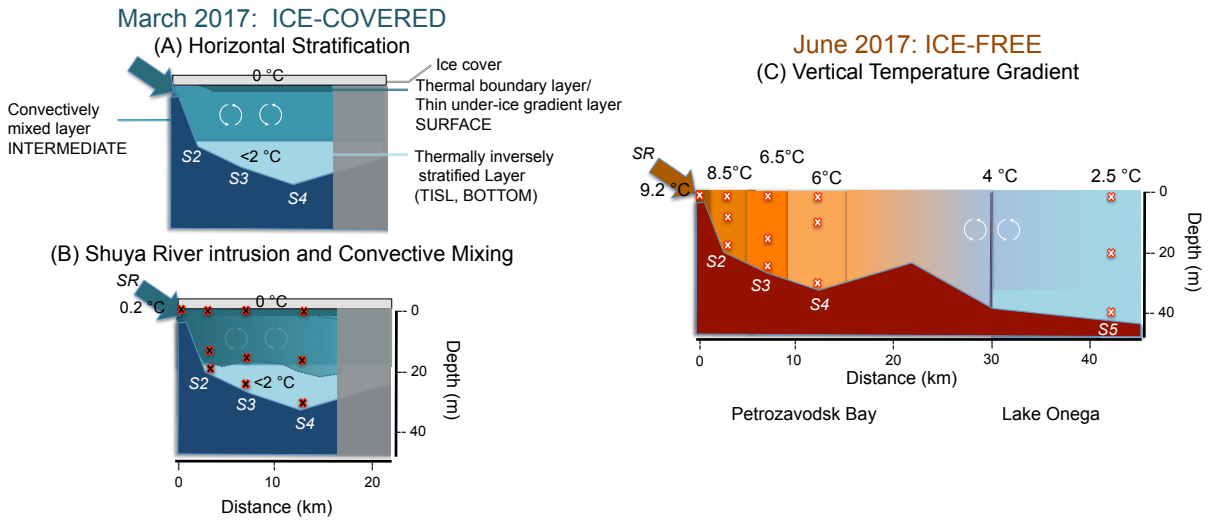


**Figure S1. Main limnological characteristics of the Bay under ice-covered (March, A, B) and ice-free conditions (June, C). Crosses indicate the depths of sampling for each sites. The figure is described in the main text and further in SI.**

Two main figures can be retained for winter limnological behaviors of the Bay. As previously described [S1], the Bay is horizontally stratified in winter, with under-ice convection promoted by higher temperature at the bottom and the influence of radiation on the snow-free ice-cover with the formation of a thin thermal boundary layer. This type of behavior has been identified in Petrozavodsk Bay in March 2015 [S2] (**Fig. S1A**). However, this convectively driven mixing is predominant solely when Shuya River inflow is low as compared to high discharge leading to river intrusion in the Bay (**Fig. S1B**). Both phenomena has been addressed in the Petrozavodsk Bay recently for March 2015 and 2016.[S3] In March 2017, the discharged was high enough for the river intrusion to occur as well.[S4] This has great influences on $CO_2$ and $CH_4$ inputs in this mixing zone during winter[S3, 4] and further on gazes atmospheric fluxes after ice-off.[S4] Lake ice-melt leads to a seasonal transition to summer stratification of the lake, as it was the case for Lake Onega in June 2015 and 2016. In June 2017 (**Fig. S1C**), the summer stratification was not established and a vertical temperature gradient due to the confluence of warm river inflow and cold lake water occurred in the Petrozadovosk Bay. Such is

characterized by the presence of a thermal bar at 4°C (maximum water density)[S5] that separate vertically the lake from the inputs of the river, the lake staying under winter inverted stratification.[S4]

## Section 2: Details regarding experimental procedures

### S2.1 Characterization of fluorogenic DOM

The excitation-emission matrices (EEMs) were used to characterize DOM fluorogenic constituents (e.g. humic-like or protein-like fluorophores).[S6] Fluorescence spectra were recorded on an LS 55 Luminescence Spectrometer (Perkin-Elmer) using a 3 mL, 1 cm path length quartz cuvette. EEMs were generated by recording emission spectra from 300 to 550 nm at 0.5 nm steps for excitation wavelengths between 200 and 450 nm with 5 nm steps. The fluorescence index (FIX),[S7] which provides information about the extent of condensation of humic substances, and thus their origin, was derived from EEM fingerprints according to: FIX = ($I_{500}/I_{450}$) for $\lambda_{Ex}$ = 370 nm. The biological index (BIX), DOM freshness, was estimated from the ratio between fluorescence intensity at $\lambda_{Em}$ =380 nm *vs* $\lambda_{Em}$ = 430 nm (BIX = $I_{380}/I_{430}$) for $\lambda_{Ex}$ = 310 nm as previously detailed.[S8] The humification index (HIX), linked to condensation degree of humic substances, was determined as the ratio of emission spectrum areas between $\lambda_{Em}$ 435–480 nm over the emission spectrum areas between $\lambda_{Em}$ 435–480 nm plus $\lambda_{Em}$ 300–345 nm (HIX= $I_{435-480}$ / ($I_{435-480} + I_{330-345}$) at $\lambda_{Ex}$ = 254 nm.[S9] Obtained values for BIX, HIX and FIX for a 10 mg $L^{-1}$ Suwannee River fulvic acid (SRFA, IHSS) gave expected values for pedogenic HS isolated from riverine DOM: 0.32, 0.96 and 1.15 for BIX, HIX, and FIX respectively. Specific UV absorbance (SUVA) at 254 nm[S10] was determined by LC-OCD, by dividing the ratio of the SAC to the respective carbon content[S11] and corrected for potential iron interferences. [S12]

**S2.2 DOM changes in composition using LC-OCD**

The organic matter constituents were characterized by size exclusion chromatography coupled in-line to a fixed wavelength detector flashing at 254nm (UVD), an organic carbon and nitrogen detector (Liquid chromatography - organic carbon detection, LC-OCD-OND (DOC-Labor Dr. Huber, Germany). The gel filtration column Toyopearl® HW-50S (Tosoh Bioscience) with a fractionation range of 20 to 0.1 kDa was used. The detection limit had been previously determined to be 10 μg C $L^{-1}$ for the OCD.[S13] Depending on their total organic contents, the samples were diluted 5 times before measurements and 2 mL injection volumes for the chromatograms were used. Samples were eluted at 1 mL $min^{-1}$ using a 24 mM phosphate buffer at pH = 6.6. DOC was further differenced in hydrophilic (HydDOC) that are separated in the column and hydrophobic DOC (HoDOC) that could not be eluted. Corresponding HydDOM components were further classified in biopolymers (BP), humic substances (HS), building blocks (BB), low molecular weight humic (LMWH), acids (LMWA) and neutral (LMWN) compounds according to their retention times and UV absorbance properties. Molecular mass distribution of the humic fraction in the samples were obtained from deconvolution of LC-OCD chromatograms using a Poisson binomal distribution shape, calibrated with SRFA ($M_n$ = 0.796 kDa) and SRHA ($M_n$ = 1.108 kDa) from whom molecular mass weight ($M_w$) and molecular mass number ($M_n$) average were obtained together with the polydispersity parameter ($D = M_w / M_n$).[S11] The aromaticity of the HS fraction, which may be expressed as the ratio of SAC to carbon, plotted against the molecular weight as $M_n$ defines the origin of the humic substances. The higher the aromaticity (SUVA) and molecularity ($M_n$) of HS, the older the water, respectively the less impact of environment, human or agriculture may be expected.[S11, 14, 15] The derivation of SUVA by LC-OCD combining separation of samples based on the size and hydrophobicity parameters for

chromogenic DOM was found to be free of iron-oxides interferences as no differences in their values were found after corrective equation[S12] and this despite quite high values of total iron (**Table S4**) we found in the samples.

**S2.3 Method for size separation of the small colloidal pool**

An AF2000 Focus (Postnova Analytics; Landsberg, Germany) was coupled to diode array and fluorescence detectors, (DAD, FLD, Postnova Analytics, Landsberg, Germany), on-line with ICPMS (model 7700x, Agilent technologies, Morges, Switzerland). A membrane with a low molecular weight cut-off (Polyestersulfone, 0.3 kDa) and high cross-flow (2.7 mL $min^{-1}$) were used for fractionation, and 10 mM $NH_4NO_3$ pH = 7 was used as eluent. The molecular mass ($M_p$) and hydrodynamic diameter ($d_h$) measured for the Shuya River by AF4-DAD were in the same order as those found for Standard Suwannee River Fulvic Acid (SRFA, $M_p$ = 1.7 kDa and $d_{hp}$ = 1.6 nm). The $M_p$ values in our studies were higher than those found for Suwannee River NOM isolate, and three different boreal river samples with $M_p$ of 0.970 kDa using the same type of instrument.[S16] This difference can be attributed to difference in separation conditions, such as: mobile phase ionic strength or pH, cross-flow programs, calibration of the channel, deconvolution of peaks or to analyte-specific properties such as the initial agglomeration state of the HS components and their origin.[S17, 18]

## Section 3: Additional figures, tables and information for main text discussion

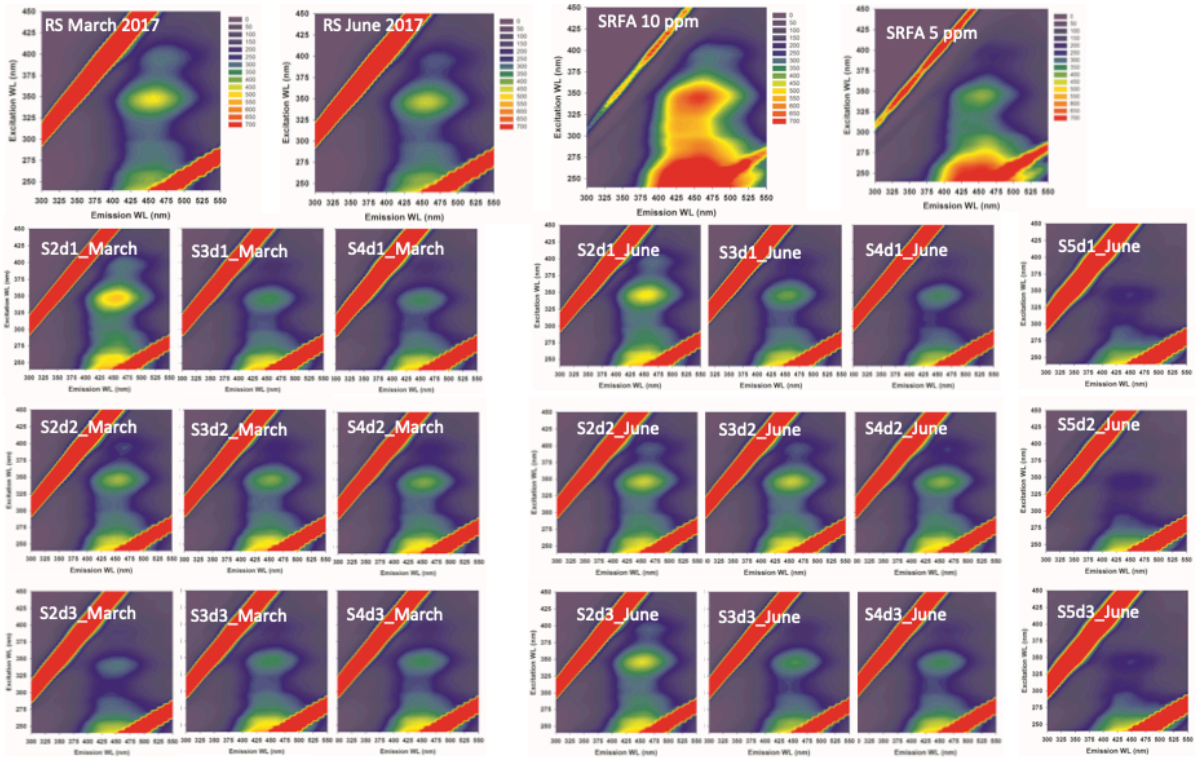


**Figure S2. Excitation-Emission Matrix (EEM) of all the samples and SRFA under the same fluorescence measurement conditions. d1, d2, and d3 referred to sampling depths respectively Surface, Intermediary and Bottom.**

**Table S2. Molecular mass characteristics of the humic components obtained by LC-OCD**

| | | ice-covered | | | | |
|---|---|---|---|---|---|---|
| | | **SR** | **S2** | **S3** | **S4** | **S5** |
| Surface | $M_n$ (Da) | 758 | 709 | 606 | 657 | |
| | $M_w$ (Da) | 4090 | 3407 | 2630 | 2726 | |
| | **D** | **5.39** | **4.81** | **4.34** | **4.15** | |
| Intermediate | $M_n$ (Da) | | 607 | 622 | 651 | |
| | $M_w$ (Da) | | 3285 | 2898 | 2891 | |
| | **D** | | **5.41** | **4.66** | **4.44** | |
| Bottom | $M_n$ (Da) | | 726 | 736 | 605 | |
| | $M_w$ (Da) | | 2644 | 2649 | 2654 | |
| | **D** | | **3.64** | **3.6** | **4.39** | |

| | | ice-free | | | | |
|---|---|---|---|---|---|---|
| | | **SR** | **S2** | **S3** | **S4** | **S5** |
| Surface | $M_n$ (Da) | 613 | 673 | 658 | 600 | 638 |
| | $M_w$ (Da) | 3088 | 3173 | 3137 | 2658 | 2087 |
| | **D** | **5.04** | **4.71** | **4.77** | **4.43** | **3.27** |
| Intermediate | $M_n$ (Da) | | 688 | 651 | 636 | 673 |
| | $M_w$ (Da) | | 3174 | 3077 | 2866 | 2260 |
| | **D** | | **4.61** | **4.73** | **4.51** | **3.36** |
| Bottom | $M_n$ (Da) | | 590 | 719 | 615 | 557 |
| | $M_w$ (Da) | | 3071 | 3188 | 2719 | 2055 |
| | **D** | | **5.21** | **4.43** | **4.42** | **3.69** |

$M_n$: number average molecular mass, $M_w$: weight average molecular mass; D: polydispersity parameter ($M_w / M_n$).

**Table S3. Molecular mass and hydrodynamic diameters of the chromophoric humic components obtained by AF4-DAD**

| | | ice-covered | | | | |
|---|---|---|---|---|---|---|
| | | **SR** | **S2** | **S3** | **S4** | **S5** |
| Surface | $M_p$ (Da) | 2028 | 1790 | 1790 | 1641 | |
| | $d_{hp}$ (nm) | 1.7 | 1.6 | 1.6 | 1.5 | |
| Intermediate | $M_p$ (Da) | | 1790 | 1790 | 1531 | |
| | $d_{hp}$ (nm) | | 1.6 | 1.6 | 1.5 | |
| Bottom | $M_p$ (Da) | | 977 | 977 | 1670 | |
| | $d_{hp}$ (nm) | | 1.2 | 1.2 | 1.5 | |

| | | ice-free | | | | |
|---|---|---|---|---|---|---|
| | | **SR** | **S2** | **S3** | **S4** | **S5** |
| Surface | $M_p$ (Da) | 2143 | 1699 | 1641 | 1302 | 1164 |
| | $d_{hp}$ (nm) | 1.7 | 1.6 | 1.5 | 1.4 | 1.3 |
| Intermediate | $M_p$ (Da) | | 1641 | 1531 | 1326 | 1164 |
| | $d_{hp}$ (nm) | | 1.5 | 1.5 | 1.4 | 1.3 |
| Bottom | $M_p$ (Da) | | 1451 | 1670 | 997 | 1164 |
| | $d_{hp}$ (nm) | | 1.5 | 1.6 | 1.2 | 1.3 |

$M_p$: molecular mass and $d_{ph}$: hydrodynamic diameter at maximum peak of absorbance recorded at $\lambda$ =254 nm by DAD (see **Figure 4**) were determined using polyestersulfonate standards for external calibration, or AF4 elution theory employing BSA as standard respectively.[S19, 20]

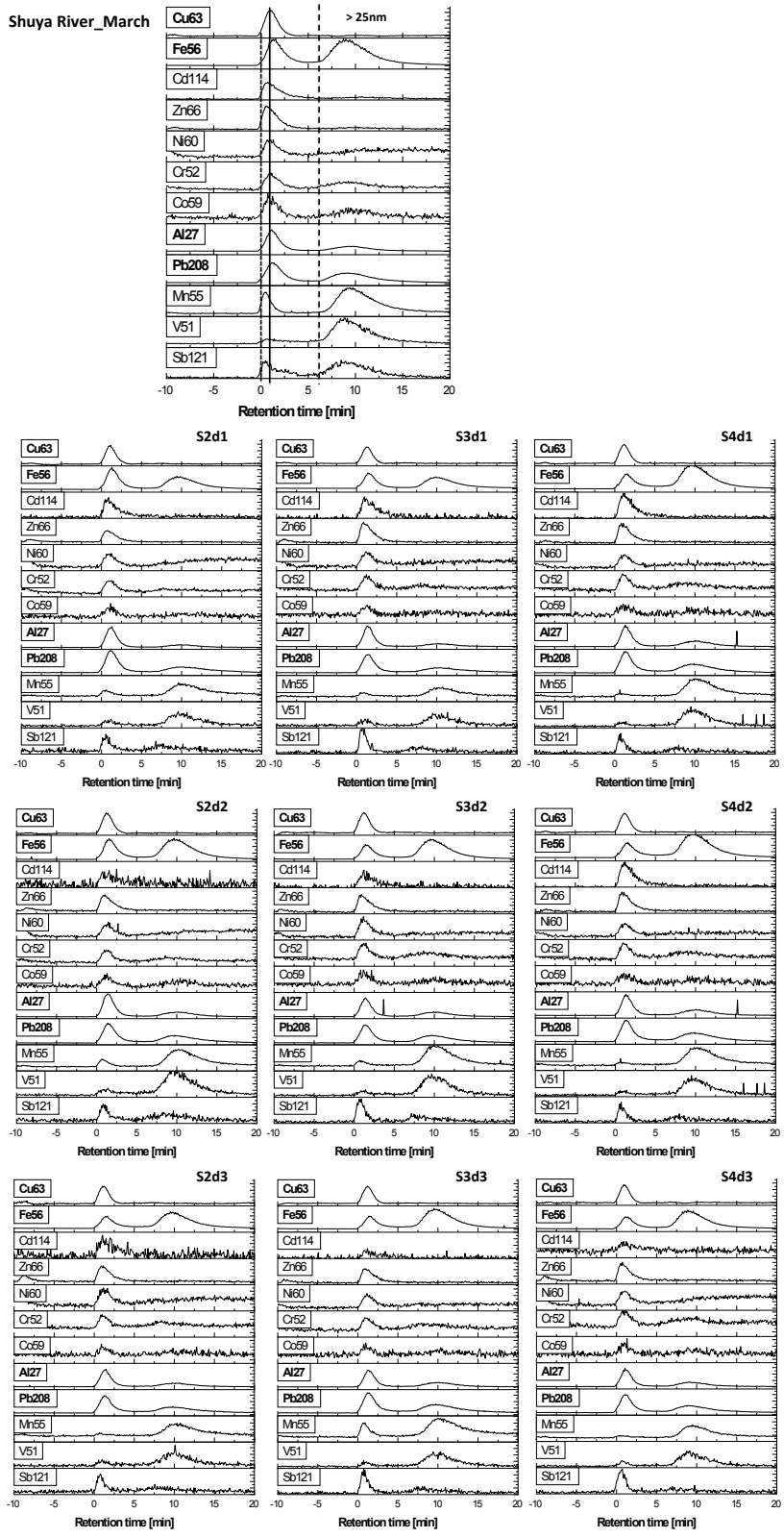


**Figure S3. Raw elemental fractograms obtained by AF4-ICPMS for the samples obtained during the ice-cover campaign**

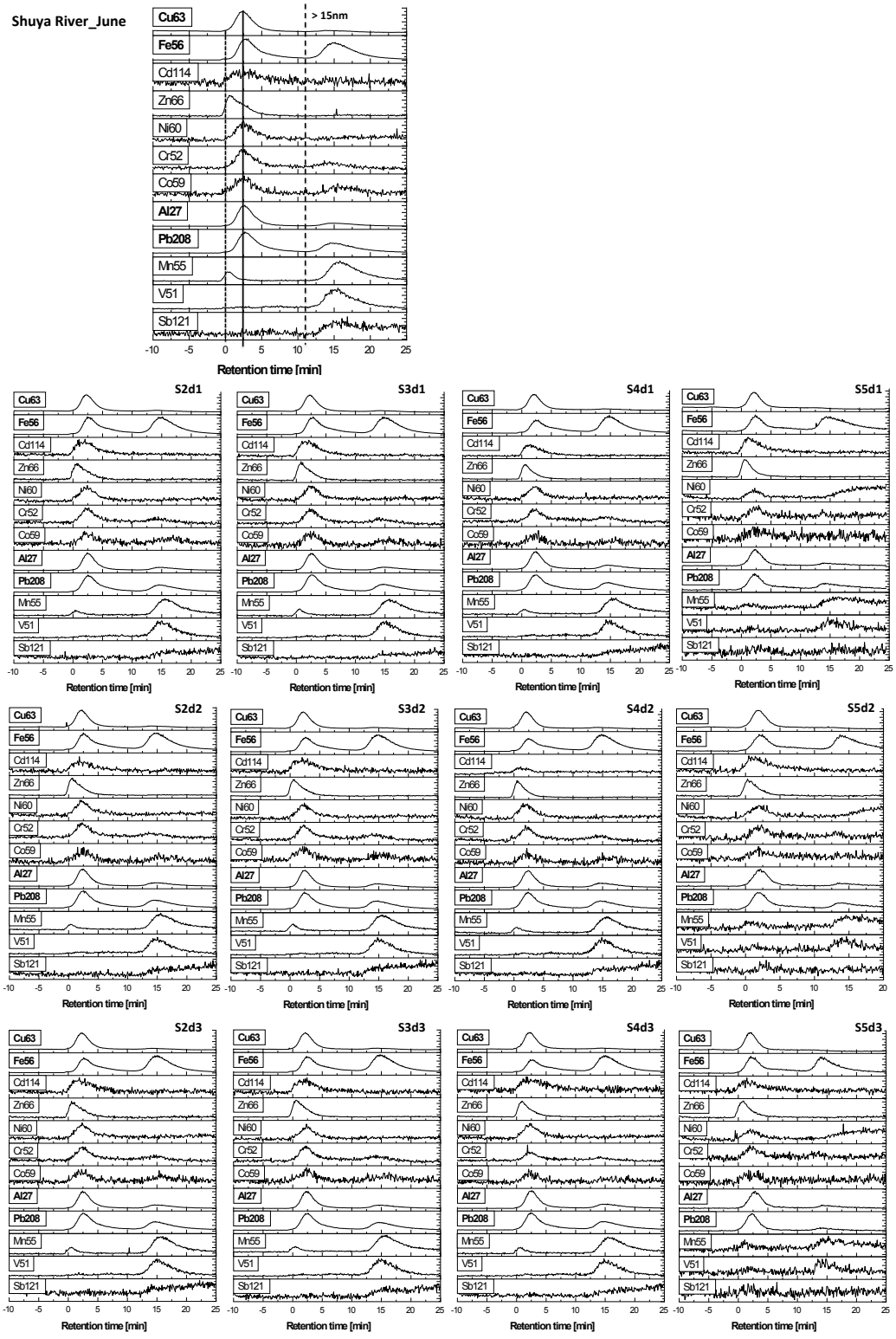


**Figure S3 (count). Figure S3. Raw elemental fractograms obtained by AF4-ICPMS for the samples obtained during the ice-free campaign**

**Supplementary informations concerning preferential binding of trace metals in the colloidal pool.**

The colloidal distribution of the metals depends on their intrinsic reactivity [S21-23] and can be grouped in our system as follows: (i) metals bound to small dissolved molecules (void, dashed lines in the **Figure S3**), and humics (HS, the elution time at peak of maximum intensity is indicated as plain line, **Figure S3**): Zn and Cd; (ii) metals bound mainly to the HS: Cu, Ni; (iii) metals bound to both humic components and large mineral colloids: Co, Cr, Al, Pb or Fe (in order of increasing association with larger colloids), and (iv) associated to or part-off large mineral colloids: Mn, V and Sb. The high Fe signal combined with low absorbance at 254 nm and fluorescence in the large colloidal pool strongly suggested the presence of iron-(hydr)-oxides, with $d_h$ > 15-25 nm in the studied waters (LIox).

For all the samples we analyze, the distribution of Cu and Ni traced the absorbance signal at 254 nm corresponding to humic substances. The Co and Cr signals were low and noisy, but their major fractions followed a similar pattern, with binding to humic substances and slight influences of iron-oxides colloids, which is consistent with the literature results for this two metals obtained with ultrafiltration.[S24] For Co, Cr, Cu and Ni, the present results are also consistent with the existing AF4 studies showing the preferential association of these metals with HS, while the elution of Pb in the larger size fraction was related to the presence of iron-oxide of small size in Alaskan rivers.[S25] While often found as truly dissolved material or as alumino-silicates,[S16] Al was found associated to HS in the Shuya River colloids. Alumino-silicates were not present in waters in of the Karelian region and Al was previously found to associate mainly with iron-oxide colloids of $M_w$ > 10 kDa or with colloids of size between 1−10 kDa and below.[S24] The size distribution of Al also depended on DOC concentration using cascade ultrafiltration for Al species < 0.2 μm.[S26] Large manganese colloids were also

likely present as Mn-oxy-hydroxides, since neither organic matter nor iron were demonstrated previously to have influence on its size distribution in rivers from this region in previous study.[S24] Both V and Sb oxyanions are found exclusively associated with LIox, contrasting with the behavior of Cr. For V our results are in agreement with those found by ultrafiltration but Sb was previously found to be mainly associated to DOM < 10 kDa in organic-rich rivers from this region.[S24] Our results for Sb also contrasted with those of a recent study showing that it did not correspond with the behavior of DOM or Fe.[S26] However the detection of Sb bound to the smaller colloidal fraction could be limited by the AF4−ICPMS method itself, because a maximum 30 % of all Sb is expected to be bound to the whole colloidal pool.[S26]

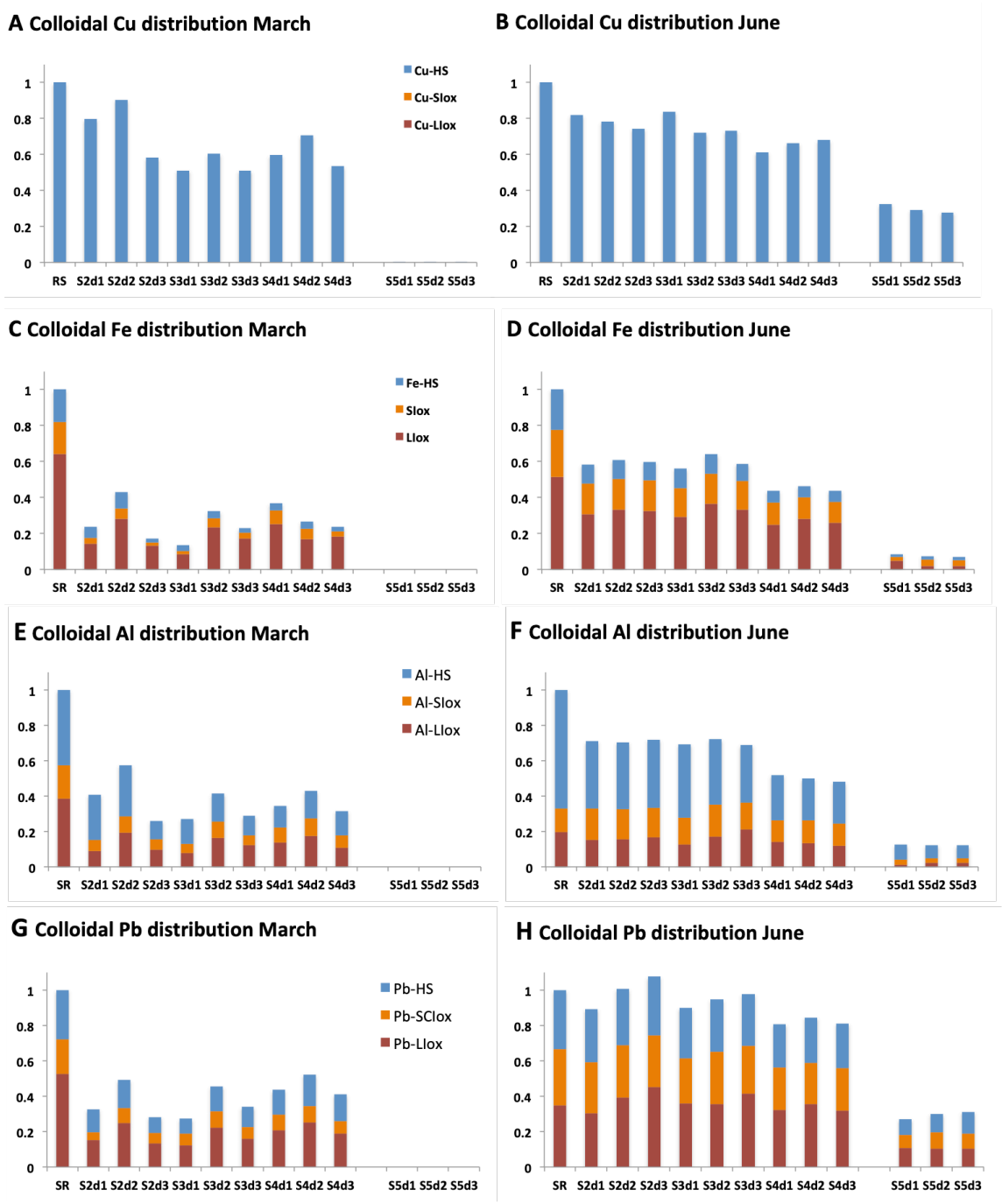


**Figure S4. Dispersion of the metallic colloidal distribution in the river–bay–lake Onega continuum for the two sampling campaigns for Cu (A, B), Fe (C, D), Al (E, F) and Pb (G, H).**

Values obtained by peaks deconvolution of the ICPMS fractograms using 3 components: metal bound to the humic components (M−HS, blue) metal bound to small iron-oxide clusters (M−SCIox, orange) and metal bound to large iron-oxides colloids (M−LIox, red). Measurements were normalized to the total colloidal content obtained in the Shuya river for each element. d1, d2, and d3 referred to sampling depths respectively Surface, Intermediary and Bottom.

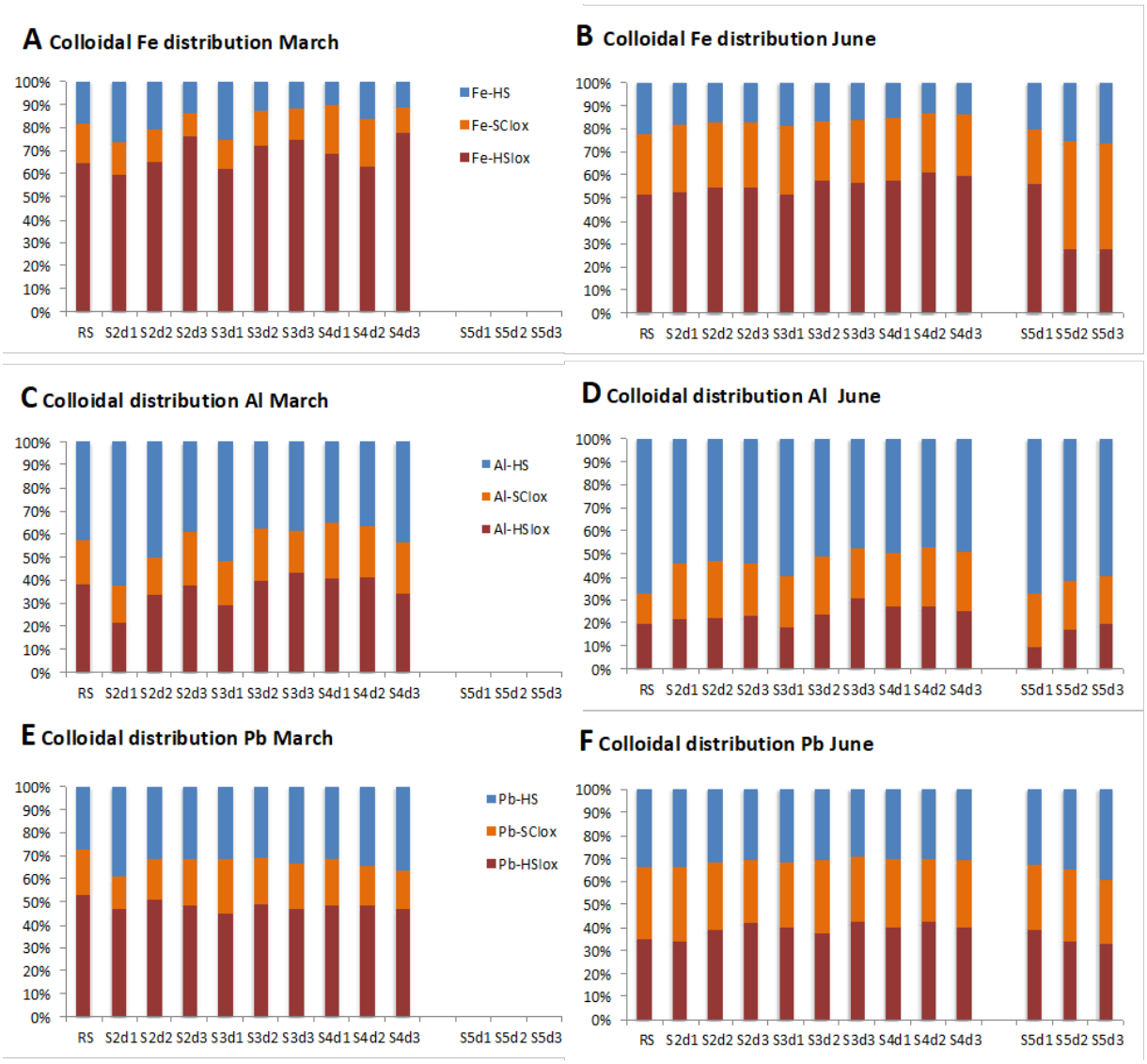


**Figure S5. Three components colloidal distribution for Fe (A, B); Al (D,E) and Pb (F,G) obtained by ICPMS fractograms deconvolution of the HS peak**. d1, d2, and d3 referred to sampling depths respectively Surface, Intermediary and Bottom.

**Table S4. Total concentrations of dissolved Fe, Al, Cu and Pb measured by ICPMS**

| | | Ice-covered | | | | |
|---|---|---|---|---|---|---|
| | | **SR** | **S2** | **S3** | **S4** | **S5** |
| **Fe (ppb)** | **d1** | **786** (33) | **453** (20) | **252** (10) | **248** (14) | |
| | **d2** | | **464** (16) | **306** (15) | **326** (12) | |
| | **d3** | | **178** (7) | **201** (7) | **248** (11) | |
| **Al (ppb)** | **d1** | **109** (4) | **72** (4) | **45** (2) | **46** (2) | |
| | **d2** | | **75** (3) | **55** (2) | **58** (2) | |
| | **d3** | | **33** (2) | **38** (2) | **50** (7) | |
| **Cu (ppb)** | **d1** | **3.2** (0.1) | **1.58** (0.07) | **1.48** (0.08) | **1.43** (0.17) | |
| | **d2** | | **0.91** (0.05) | **1.26** (0.36) | **1.37** (0.07) | |
| | **d3** | | **1.05** (0.08) | **1.01** (0.11) | **1.14** (0.06) | |
| **Pb (ppb)** | **d1** | **0.45** (0.02) | **0.34** (0.03) | **0.25** (0.00) | **0.16** (0.00) | |
| | **d2** | | **0.27** (0.01) | **0.18** (0.01) | **0.19** (0.00) | |
| | **d3** | | **0.14** (0.01) | **0.13** (0.01) | **0.16** (0.04) | |

| | | Ice-free | | | | |
|---|---|---|---|---|---|---|
| | | **SR** | **S2** | **S3** | **S4** | **S5** |
| **Fe (ppb)** | **d1** | **647** (31) | **272** (1) | **370** (1) | **289** (10) | **29** (1) |
| | **d2** | | **303** (4) | **387** (9) | **287** (3) | **28** (1) |
| | **d3** | | **404** (20) | **327** (11) | **268** (4) | **32** (1) |
| **Al (ppb)** | **d1** | **142** (9) | **87** (1) | **91** (1) | **67** (2) | **10** (1) |
| | **d2** | | **85** (1) | **91** (0) | **66** (1) | **11** (0) |
| | **d3** | | **97** (3) | **77** (2) | **63** (1) | **10** (0) |
| **Cu (ppb)** | **d1** | **3** (2) | **3.99** (0.01) | **3.59** (-) | **3.10** (0.14) | **3.21** (0.13) |
| | **d2** | | **2.66** (0.05) | **2.14** (0.41) | **2.19** (0.06) | **1.80** (0.01) |
| | **d3** | | **2.84** (0.58) | **2.31** (0.10) | **1.76** (0.57) | **1.67** (0.05) |
| **Pb (ppb)** | **d1** | **0.78** (0.34) | **0.36** (0.02) | **0.38** (0.01) | **0.47** (0.01) | **0.24** (0.04) |
| | **d2** | | **0.35** (0.00) | **0.40** (0.09) | **0.31** (0.00) | **0.21** (0.06) |
| | **d3** | | **0.78** (0.14) | **0.28** (0.02) | **0.24** (0.03) | **0.20** (0.05) |

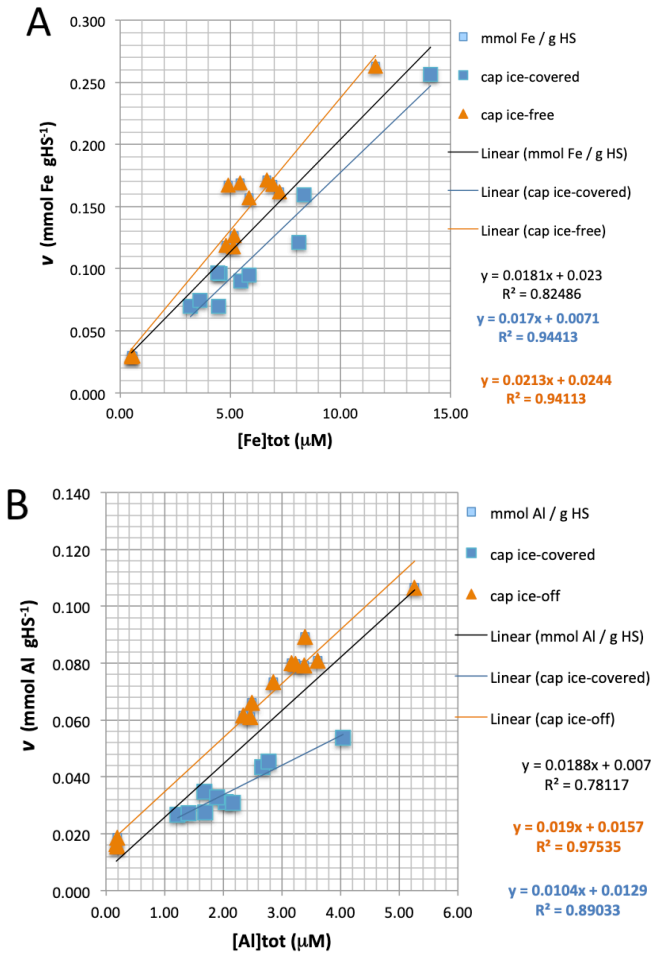


**Figure S6. Fe (A) and Al (B) binding capacities as the function of total dissolved metals.**

**References**


S1. Kirillin, G.; Leppäranta, M.; Terzhevik, A.; Granin, N.; Bernhardt, J.; Engelhardt, C.; Efremova, T.; Golosov, S.; Palshin, N.; Sherstyankin, P.; Zdorovennova, G.; Zdorovennov, R., Physics of seasonally ice-covered lakes: a review. *Aquatic Sciences* **2012,** *74*, (4), 659-682.

S2. Bouffard, D.; Zdorovennov, R. E.; Zdorovennova, G. E.; Pasche, N.; Wuest, A.; Terzhevik, A. Y., Ice-covered Lake Onega: effects of radiation on convection and internal waves. *Hydrobiologia* **2016,** *780*, (1), 21-36.

S3. Pasche, N.; Hofmann, H.; Bouffard, D.; Schubert, C. J.; Lozovik, P. A.; Sobek, S., Implications of river intrusion and convective mixing on the spatial and temporal variability of under-ice CO2. *Inland Waters* **2019,** *9*, (2), 162-176.

S4. Chmiel, H. E.; Hofmann, H.; Sobek, S.; Efremova, T.; Pasche, N., Where does the river end? Drivers of spatiotemporal variability in CO2 distribution and flux in the inflow area of a large boreal lake. *Limnology and Oceanography,* **accepted**.

S5. Holland, P. R.; Kay, A., A review of the physics and ecological implications of the thermal bar circulation. *Limnologica* **2003,** *33*, (3), 153-162.

S6. Worms, I. A. M.; Slaveykova, V. I.; Wilkinson, K. J., Lead Bioavailability to Freshwater Microalgae in the Presence of Dissolved Organic Matter: Contrasting Effect of Model Humic Substances and Marsh Water Fractions Obtained by Ultrafiltration. *Aquatic Geochemistry* **2015,** *21*, (2-4), 217-230.

S7. McKnight, D. M.; Boyer, E. W.; Westerhoff, P. K.; Doran, P. T.; Kulbe, T.; Andersen, D. T., Spectrofluorometric characterization of dissolved organic matter for indication of precursor organic material and aromaticity. *Limnology and Oceanography* **2001,** *46*, (1), 38-48.

S8. Huguet, A.; Vacher, L.; Relexans, S.; Saubusse, S.; Froidefond, J. M.; Parlanti, E., Properties of fluorescent dissolved organic matter in the Gironde Estuary. *Organic Geochemistry* **2009,** *40*, (6), 706-719.

S9. Zsolnay, A.; Baigar, E.; Jimenez, M.; Steinweg, B.; Saccomandi, F., Differentiating with fluorescence spectroscopy the sources of dissolved organic matter in soils subjected to drying. *Chemosphere* **1999,** *38*, (1), 45-50.

S10. Weishaar, J. L.; Aiken, G. R.; Bergamaschi, B. A.; Fram, M. S.; Fujii, R.; Mopper, K., Evaluation of Specific Ultraviolet Absorbance as an Indicator of the Chemical Composition and Reactivity of Dissolved Organic Carbon. *Environ. Sci. Technol.* **2003,** *37*, (20), 4702-4708.

S11. Huber, S. A.; Balz, A.; Abert, M.; Pronk, W., Characterisation of aquatic humic and non-humic matter with size-exclusion chromatography – organic carbon detection – organic nitrogen detection (LC-OCD-OND). *Water Research* **2011,** *45*, (2), 879-885.

S12. Poulin, B. A.; Ryan, J. N.; Aiken, G. R., Effects of Iron on Optical Properties of Dissolved Organic Matter. *Environ. Sci. Technol.* **2014,** *48*, (17), 10098-10106.

S13. Huber, S. A.; Frimmel, F. H., Flow injection analysis for organic and inorganic carbon in the low-ppb range. *Analytical Chemistry* **1991,** *63*, (19), 2122-2130.

S14. Stewart, T. J.; Traber, J.; Kroll, A.; Behra, R.; Sigg, L., Characterization of extracellular polymeric substances (EPS) from periphyton using liquid chromatography-organic carbon detection–organic nitrogen detection (LC-OCD-OND). *Environmental Science and Pollution Research* **2013,** *20*, (5), 3214-3223.

S15. Velten, S.; Knappe, D. R. U.; Traber, J.; Kaiser, H.-P.; von Gunten, U.; Boller, M.; Meylan, S., Characterization of natural organic matter adsorption in granular activated carbon adsorbers. *Water Research* **2011,** *45*, (13), 3951-3959.
S16. Cuss, C. W.; Grant-Weaver, I.; Shotyk, W., AF4-ICPMS with the 300 Da Membrane To Resolve Metal-Bearing "Colloids" < 1 kDa: Optimization, Fractogram Deconvolution, and Advanced Quality Control. *Analytical Chemistry* **2017,** *89*, (15), 8027-8035.
S17. Cuss, C. W.; Guéguen, C., Determination of relative molecular weights of fluorescent components in dissolved organic matter using asymmetrical flow field-flow fractionation and parallel factor analysis. *Analytica Chimica Acta* **2012,** *733*, 98-102.
S18. Cuss, C. W.; Guéguen, C., Distinguishing dissolved organic matter at its origin: Size and optical properties of leaf-litter leachates. *Chemosphere* **2013,** *92*, (11), 1483-1489.
S19. Worms, I. A. M.; Adenmatten, D.; Miéville, P.; Traber, J.; Slaveykova, V. I., Photo-transformation of pedogenic humic acid and consequences for Cd(II), Cu(II) and Pb(II) speciation and bioavailability to green microalga. *Chemosphere* **2015,** *138*, 908-915.
S20. Worms, I. A. M.; Al-Gorani Szigeti, Z.; Dubascoux, S.; Lespes, G.; Traber, J.; Sigg, L.; Slaveykova, V. I., Colloidal organic matter from wastewater treatment plant effluents: Characterization and role in metal distribution. *Water Research* **2010,** *44*, (1), 340-350.
S21. Wilkinson, K. J.; Lead, J. R., *Environmental Colloids and Particles. Behaviour, Separation and Characterisation*. John Wiley Sons, Ltd. Chichester, UK: 2007; Vol. 10.
S22. Tercier Waeber, M., Stoll, S., & Slaveykova, V. , Trace metal behavior in surface waters: Emphasis on dynamic speciation, sorption processes and bioavailability. *Archives Des Sciences* **2012,** *65*, 119-142.
S23. Lyvén, B.; Hassellöv, M.; Turner, D. R.; Haraldsson, C.; Andersson, K., Competition between iron- and carbon-based colloidal carriers for trace metals in a freshwater assessed using flow field-flow fractionation coupled to ICPMS. *Geochimica et Cosmochimica Acta* **2003,** *67*, (20), 3791-3802.
S24. Pokrovsky, O. S.; Schott, J., Iron colloids/organic matter associated transport of major and trace elements in small boreal rivers and their estuaries (NW Russia). *Chemical Geology* **2002,** *190*, (1-4), 141-179.
S25. Stolpe, B.; Guo, L.; Shiller, A. M.; Aiken, G. R., Abundance, size distributions and trace-element binding of organic and iron-rich nanocolloids in Alaskan rivers, as revealed by field-flow fractionation and ICP-MS. *Geochimica et Cosmochimica Acta* **2013,** *105*, 221-239.
S26. Ilina, S. M.; Lapitskiy, S. A.; Alekhin, Y. V.; Viers, J.; Benedetti, M.; Pokrovsky, O. S., Speciation, Size Fractionation and Transport of Trace Elements in the Continuum Soil Water–Mire–Humic Lake–River–Large Oligotrophic Lake of a Subarctic Watershed. *Aquatic Geochemistry* **2016,** *22*, (1), 65-95.